

Fano factor and nonuniformities affecting charge transport in semiconductors

M. J. Harrison and D. S. McGregor
Kansas State University, Manhattan, Kansas 66502, USA

F. P. Doty
Sandia National Laboratories, Livermore, California 94551, USA

(Received 14 December 2007; revised manuscript received 26 March 2008; published 19 May 2008)

The Fano factor is a measure of the variance in the number of charge carriers produced in materials by ionizing radiation interactions, which determines the ultimate energy resolution achievable by a semiconductor spectrometer. Similar to charge production, charge transport in semiconductors suffers variation due to material nonuniformities. A reanalysis of published data illustrates that the variance in electron drift length, which is typically neglected in the estimation of the Fano factor, is significant for CdZnTe. In fact, at low electric fields, signal variance due to inhomogeneous charge transport can dominate. Our analysis shows that the standard deviation in the electron drift length is on the order of hundreds of microns for the published data.

DOI: [10.1103/PhysRevB.77.195207](https://doi.org/10.1103/PhysRevB.77.195207)

PACS number(s): 72.20.Jv

I. INTRODUCTION

Fano¹ first assumed a constant of proportionality in 1947 to estimate the deviation from Poisson statistics that was observed between the mean of and the variance in the number of ions produced in a gas from an ionizing radiation interaction. Poisson statistics prescribes that the variance is equal to the mean. This constant of proportionality has since become known as the Fano factor F and is defined as

$$F = \frac{\sigma_N^2}{\bar{N}}, \quad (1)$$

where σ_N^2 is the variance in the number of charges produced per event and \bar{N} is the average number of charges produced. For true Poisson statistics, $F=1$. However, errors in any practical measurement of the Fano factor in a process that is strictly governed by Poisson statistics will always produce $F > 1$, such that $F=1$ becomes a lower bound for any measurement of the Fano factor for a true Poisson process. Ionization and charge pair creation clearly deviate from Poisson statistics; thus, values of $F < 1$ are commonly measured.

Originally meant for gases wherein $F \approx 0.4$,¹ the convention was later adopted for semiconductors as both types of material clearly deviate from Poisson statistics. In semiconductors, the Fano factor is typically estimated to be on the order of 0.1 (see, e.g. Ref. 2).

It is interesting to note that the measurement and theoretical prediction of the Fano factor was a popular topic for many years (see, e.g., Refs. 2–19). This was followed in the 1980s with little or no activity on the topic. Only recently has the research community regained interest in the Fano factor (see, e.g., Refs. 20–33).

The Fano factor in semiconductor materials is typically estimated from the measurements of photopeak widths and electronic noise by using x-ray spectrometers. These spectrometers are typically thin samples of an undoped semiconductor material with an externally applied electric field. Some experimentalists choose to use p - n or p - i - n diodes instead, but those will not be considered in the following

derivations as they suffer from nonconstant internal electric fields, thus greatly complicating the analysis.

A typical Fano factor measurement consists of arranging an x-ray spectrometer such that low energy, monoenergetic x-rays interact near the cathode of the device. Each x-ray entering the semiconductor photoelectrically transfers its energy to an electron in the valence or lower shell. The excited electron, or rather “hot” electron, then travels through the bulk of the semiconductor, elastically and inelastically scattering with other valence electrons and exciting them into the conduction band of the semiconductor. The excited electrons are drifted through the semiconductor bulk toward the anode. As they drift, a mirror charge is induced on the anode by forming a current pulse, which can then be measured by using a multichannel analyzer (MCA). A MCA bins each interaction according to the magnitude of the current pulse. The variance in the measured pulses is assumed to be the sum of the variances in the charge creation and electronic noise, thus allowing for a simple calculation of the Fano factor.

Unfortunately, in all of the work done on the topic, a simplifying assumption has been made that the variances in the charge transport properties and electric field are negligible in comparison to the variances in the charge production. Some authors recognized that an increased electric field improves the charge collection and, thus, decreases the relative importance of charge transport variances.^{2,9,12,19,23,31–33} Nevertheless, the authors assumed these collection variances to be negligible at high electric fields or used estimates in determining the Fano factor.

In its simplest form, the observed photopeak widths are expressed as a sum of three independent variances,

$$\sigma_{\text{tot}}^2 = \sigma_N^2 + \sigma_e^2 + \sigma_{\text{elect}}^2, \quad (2)$$

where σ_{tot}^2 is the total measured variance in a monoenergetic x-ray full energy peak, σ_e^2 is the variance in the collection efficiency, and σ_{elect}^2 is the signal variance due to electronic noise. Typically, σ_e^2 is assumed negligible and the variance in the charge pair creation is calculated as the difference between the total and electronic variances.

The review of literature on Si and Ge suggests that it is prudent to realize the importance of transport variance, especially for materials that are relatively “young.” Nonuniformities necessarily affect the charge transport, thus increasing the estimated Fano factor value. This heuristic argument may explain why the reported Fano factor values for Si and Ge continued to drop as the crystal growth technology for these materials matured.

This work develops the explicit mathematical equations for the variances in semiconductor materials. By using CdZnTe as an example, the importance of material homogeneity will be analyzed below.

II. ERROR PROPAGATION ANALYSIS

The amount of charge induced on an electrode Q due to an interaction in the bulk of a semiconductor creating \bar{N} free charge pairs can be modeled as

$$Q = q\bar{N}\varepsilon(x, \mathbf{E}), \quad (3)$$

where q is the elementary charge and $\varepsilon(x, \mathbf{E})$ is the charge collection efficiency of the device at an interaction location x and at an average applied electric field \mathbf{E} . For an infinite planar detector, the Hecht equation accurately describes the mean charge collection efficiency as

$$\varepsilon(x, \mathbf{E}) = \frac{\lambda_h}{L} \left[1 - \exp\left(\frac{-x}{\lambda_h}\right) \right] + \frac{\lambda_e}{L} \left[1 - \exp\left(\frac{x-L}{\lambda_e}\right) \right], \quad (4)$$

where

$$\lambda_h = \mu\tau_h\mathbf{E}, \quad (5)$$

and

$$\lambda_e = \mu\tau_e\mathbf{E}. \quad (6)$$

λ_h and λ_e are called the hole and electron drift lengths, respectively. L is the entire length of the active region of the detector and $\mu\tau_h$ and $\mu\tau_e$ are the hole and electron mobility lifetime products, respectively.

After propagating errors through Eq. (3), the charge variance is found to be

$$\sigma_Q^2 = \left(\frac{\partial Q}{\partial \bar{N}} \right)^2 \sigma_{\bar{N}}^2 + \left(\frac{\partial Q}{\partial \varepsilon} \right)^2 \sigma_\varepsilon^2, \quad (7)$$

in which σ_ε^2 is the variance in the charge collection efficiency. To determine σ_ε^2 , we propagate errors through Eq. (4) to find

$$\sigma_\varepsilon^2 = \left(\frac{\partial \varepsilon}{\partial \lambda_h} \right)^2 \sigma_{\lambda_h}^2 + \left(\frac{\partial \varepsilon}{\partial \lambda_e} \right)^2 \sigma_{\lambda_e}^2 + \left(\frac{\partial \varepsilon}{\partial x} \right)^2 \sigma_x^2, \quad (8)$$

where

$$\frac{\partial \varepsilon}{\partial \lambda_h} = \frac{1}{L} \left\{ \left[1 - \exp\left(\frac{-x}{\lambda_h}\right) \right] - \frac{x}{\lambda_h} \exp\left(\frac{-x}{\lambda_h}\right) \right\}, \quad (9)$$

$$\frac{\partial \varepsilon}{\partial \lambda_e} = \frac{1}{L} \left\{ \left[1 - \exp\left(\frac{x-L}{\lambda_e}\right) \right] + \frac{x-L}{\lambda_e} \exp\left(\frac{x-L}{\lambda_e}\right) \right\}, \quad (10)$$

and

$$\frac{\partial \varepsilon}{\partial x} = \frac{1}{L} \left[\exp\left(\frac{-x}{\lambda_h}\right) - \exp\left(\frac{x-L}{\lambda_e}\right) \right]. \quad (11)$$

Now, we suppose that the planar detector is irradiated by low energy x rays at the cathode. Since the attenuation coefficient is high for low energy x rays, nearly all interactions occur very near the cathode surface, i.e., at $x \approx 0$. For this case, two key approximations can be made.

Approximation 1:

$$\left(\frac{\partial \varepsilon}{\partial x} \right)^2 \sigma_x^2 \approx 0 \quad \text{since both} \quad \left. \left(\frac{\partial \varepsilon}{\partial x} \right) \right|_{x=0} \ll 1 \quad \text{and} \quad \sigma_x \ll 1. \quad (12)$$

Approximation 2:

$$\left(\frac{\partial \varepsilon}{\partial \lambda_h} \right) \approx 0 \quad \text{since} \quad \lim_{x \rightarrow 0} \left(\frac{\partial \varepsilon}{\partial \lambda_h} \right) = 0. \quad (13)$$

Simplifying Eq. (8) with the approximations in Eqs. (12) and (13), substituting Eq. (10), and setting $x=0$ yields

$$\sigma_\varepsilon^2 = \left(\frac{1}{L} \left\{ \left[1 - \exp\left(\frac{-L}{\lambda_e}\right) \right] + \frac{-L}{\lambda_e} \exp\left(\frac{-L}{\lambda_e}\right) \right\} \right)^2 \sigma_{\lambda_e}^2. \quad (14)$$

After performing the differentiation in Eq. (7), the collected charge variance is found to be

$$\sigma_Q^2 = (q\varepsilon)^2 F\bar{N} + (q\bar{N})^2 \left(\frac{\partial \varepsilon}{\partial \lambda_e} \right)^2 \sigma_{\lambda_e}^2. \quad (15)$$

Equation (15) has important implications for experimentally determining the Fano factor in a semiconductor. Since both ε and $\partial\varepsilon/\partial\lambda_e$ depend on the electric field, the signal variance is also electric field dependent. Upon inspection, it is seen that the overall charge variance is simply the sum of two independent equations. Let

$$A(\mathbf{E}) = (q\varepsilon)^2 \bar{N}, \quad (16)$$

$$B(\mathbf{E}) = (q\bar{N})^2 \left(\frac{\partial \varepsilon}{\partial \lambda_e} \right)^2, \quad (17)$$

and assume, for now, that F and $\sigma_{\lambda_e}^2$ are constant with respect to the electric field strength. Equation (15) can then be rewritten as

$$\sigma_Q^2 = FA(\mathbf{E}) + \sigma_{\lambda_e}^2 B(\mathbf{E}). \quad (18)$$

The two electric field dependent functions $A(\mathbf{E})$ and $B(\mathbf{E})$ have distinct relationships with \mathbf{E} . It can be observed from the substitution of Eqs. (4), (10), (16), and (17) into Eq. (18) that the value of the “Fano term” increases as the electric field is increased and that the “electron drift term” decreases with increasing electric field. Figure 1 illustrates this rela-

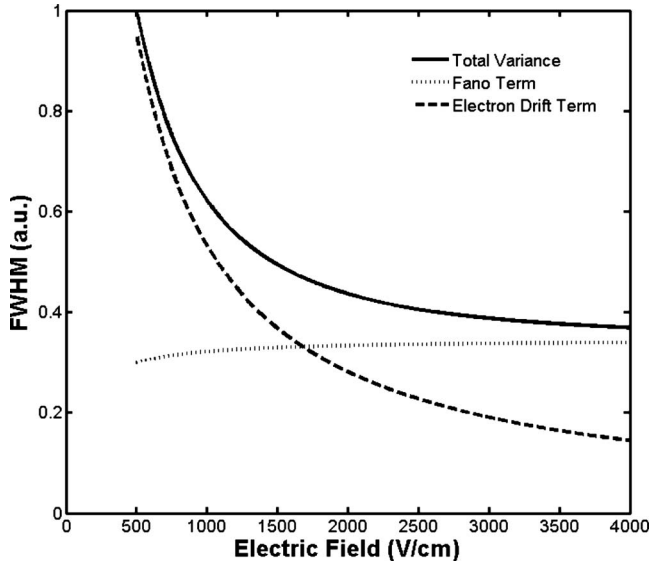


FIG. 1. Dependency of each term in Eq. (18) on the electric field. Note that the Fano term increases with increasing electric field strength, while the electron drift term decreases with increasing electric field strength. It is assumed here that electronic noise contribution is zero.

relationship for a sample of $L=0.15$ cm and with an electron mobility lifetime product of $\mu\tau_e=1 \times 10^{-3}$ $\text{cm}^2 \text{V}^{-1}$. This is an important result in the relationship that the experimentally measured values of σ_Q^2 with an applied electric field is an indicator of relative importance of these two terms, $A(\mathbf{E})$ and $B(\mathbf{E})$. Furthermore, a multivariate minimization algorithm could be employed to estimate the values of F and $\sigma_{\lambda_e}^2$.

III. LITERATURE DATA ANALYSIS

Two published data sets meet the requirements as set forth in the assumptions of Eqs. (12) and (13). In 1994, Niemelä and Sipilä²³ performed measurements on a $5 \times 5 \times 1.5$ mm^3 planar cadmium zinc telluride ($\text{Cd}_{0.8}\text{Zn}_{0.2}\text{Te}$) x-ray/gamma-ray spectrometer ($L=0.15$ cm) and in 1998, Redus *et al.*²⁹ performed similar measurements on a $3 \times 3 \times 2$ mm^3 $\text{Cd}_{0.8}\text{Zn}_{0.2}\text{Te}$ spectrometer ($L=0.2$ cm). Both data sets are provided in Table I. These experiments used the $K\alpha$ x ray of ^{55}Fe , which has an energy of 5.9 keV. The average energy necessary to create one electron-hole pair in $\text{Cd}_{0.8}\text{Zn}_{0.2}\text{Te}$ was estimated to be 5.0 eV;^{23,29} thus, it is expected that $\bar{N}=1180$ pairs. The electron mobility for both devices is assumed to be 1000 $\text{cm}^2 \text{V}^{-1} \text{s}^{-1}$. The electron trapping times are estimated to have been on the order of 1 μs .

A line of best fit was calculated for each set of data by fitting Eq. (17) via a simplex algorithm that adjusted F and $\sigma_{\lambda_e}^2$ to minimize the root mean square error Err between the experimental data and the theoretically predicted value of the full width at half maximum (FWHM) as given in Eq. (19),

$$\text{Err} = \sqrt{\sum(\sigma_{Qx}^2 - \sigma_{Qp}^2)}, \quad (19)$$

where σ_{Qx}^2 is the experimentally measured net signal variance and σ_{Qp}^2 is the net signal variance as predicted by Eq.

TABLE I. Previously published net variance in collected charge values. The listed values are net variance and were found by subtracting the measured electronic variances from the total variances. The values are from Refs. 23 and 29.

Data set	Electric field (E) (V/cm)	Electron drift length (D_e) (cm)	Measured FWHM (eV)
Ref. 23	1 333	1.33	461.0
	2 667	2.67	253.6
	4 000	4.00	215.9
	5 333	5.33	186.6
	6 667	6.67	135.7
Ref. 29	1 250	1.25	146.7
	1 500	1.50	134.9
	1 750	1.75	128.9
	2 000	2.00	123.4
	2 250	2.25	123.4

(18). It is unfortunate that the necessary data for a proper error analysis are unavailable in Refs. 23 and 29.

IV. RESULTS

The minimum Fano factor calculated for $\text{Cd}_{0.8}\text{Zn}_{0.2}\text{Te}$ was 0.074. Fitting the experimental data with this value yields electron drift standard deviation σ_{λ_e} values of 237 and 53 μm for the data sets of Niemelä and Sipilä²³ and Redus *et al.*,²⁹ respectively. Figure 2 plots the two terms of Eq. (17), the total theoretical variance, and the data points for the data

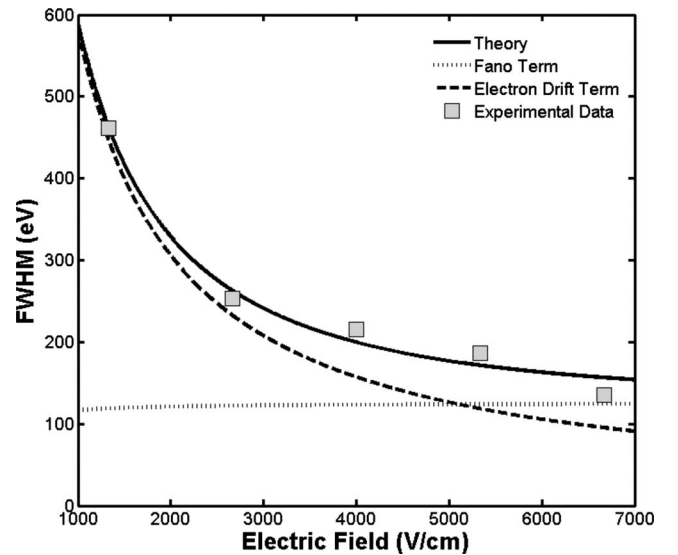


FIG. 2. Theoretical line of best fit to the data set of Niemelä and Sipilä (Ref. 23). Note that the electron drift term dominates the observed variance until the electric field becomes greater than ~ 5500 V/cm. A two-term fit yields $F=0.097$ and $\sigma_{\lambda_e}^2=5.4 \times 10^{-4}$ cm^2 with $R^2=0.998$. Niemelä and Sipilä (Ref. 23) reported a Fano factor value of 0.14.

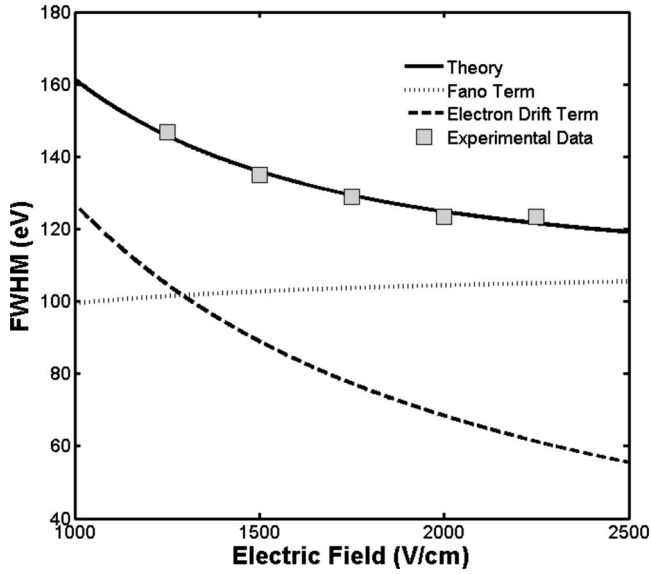


FIG. 3. Theoretical line of best fit to data set of Redus *et al.* (Ref. 29). Note here that the electron drift term does not dominate the observed variance until the electric field drops below ~ 1300 V/cm. A two-term best fit model yields $F=0.074$ and $\sigma_{\lambda_e}^2=2.8 \times 10^{-5}$ cm² with $R^2=0.973$. Redus *et al.* (Ref. 29) reported a Fano factor value of 0.089 ± 0.005 with a minimum observed value of 0.082.

set of Niemelä and Sipilä.²³ Figure 3 plots the same for the data of Redus *et al.*²⁹

To ensure that the simplex algorithm did actually find the minimum of Eq. (19) and not simply a local minimum, \mathbf{E} was plotted in a contour plot over the physically possible parameter space. For values of $0 \leq F \leq 1$ and $10^{-8} \leq \sigma_{\lambda_e}^2 \leq 10^8$ cm² and perhaps beyond, there exists only one minimum for both data sets.

V. DISCUSSION

Error propagation analysis was used to explicitly express material inhomogeneity terms in the charge collection model of an infinite planar semiconductor detector. The derived function [Eq. (17)] fits the experimental results quite well. This fact indicates that the assumption that the electron drift variance is independent of the electric field was valid. If this is indeed the case, then further conclusions can be drawn from this result.

The electron drift length is defined in Eq. (5). Propagating errors through this equation yields another expression for $\sigma_{\lambda_e}^2$. It is

$$\sigma_{\lambda_e}^2 = \left(\frac{\partial \lambda_e}{\partial \mu \tau_e} \right)^2 \sigma_{\mu \tau_e}^2 + \left(\frac{\partial \lambda_e}{\partial \mathbf{E}} \right)^2 \sigma_{\mathbf{E}}^2. \quad (20)$$

Here, the electron drift variance is broken into two parts. One part is due to variances in the mobility-lifetime product of electrons $\sigma_{\mu \tau_e}^2$ and a second term is due to local variances in the electric field $\sigma_{\mathbf{E}}^2$. In the case of CdZnTe, it is well known that Te precipitates can act as charge traps.³⁴ It is also very probable that these precipitates disturb the electric field

nearby. Furthermore, hot electrons passing through the precipitates are likely to experience a deviation in stopping power due to material differences, which in turn affects the variation in the number of charge carrier pairs produced per unit energy. Therefore, it is expected that the presence of precipitates in a crystal, such as those seen in CdZnTe, affect both the variance in charge pair creation and the variance in charge transport by trapping the charge carriers and distorting the local electric field. Moreover, it is therefore posited that the Fano factor is material quality dependent.

If we again look at Eq. (18), specifically at \bar{N} , we find that the Fano term can be further split into two parts. \bar{N} is commonly modeled as

$$\bar{N} = \frac{E_\gamma}{\beta E_g}, \quad (21)$$

where E_γ is the energy deposited in the device by the photon, E_g is the band gap energy of the semiconductor, and β is a constant relating the number of charges that is produced to the band gap energy. After propagating errors through Eq. (21), two important terms come to the forefront,

$$\sigma_N^2 = \left(\frac{\partial \bar{N}}{\partial \beta} \right)^2 \sigma_\beta^2 + \left(\frac{\partial \bar{N}}{\partial E_g} \right)^2 \sigma_{E_g}^2. \quad (22)$$

The first term, $(\partial \bar{N} / \partial \beta)^2 \sigma_\beta^2$, represents the intrinsic variances in the amount of energy required to produce an electron-hole pair in the semiconductor; while the second, $(\partial \bar{N} / \partial E_g)^2 \sigma_{E_g}^2$, represents a material-dependent variance in the band gap energy. In elemental semiconductors, such as Si or Ge, the second term is likely negligible, but for a ternary compound semiconductor, such as CdZnTe, the second term has meaning since Zn concentration determines the band gap energy. Unfortunately, since both terms of Eq. (22) have the same dependence on the electric field, it is impossible to separate the two terms and determine the relative importance of the two terms in determining the overall variance with the available datasets. Tight control of the band gap energy over several samples may, in the future, elucidate the difference between the two. For now, the variances due to material inhomogeneities and intrinsic variances from energy band statistics are inseparable, thus potentially explaining the differences in measured Fano factor values.

VI. CONCLUSIONS

In summary, it was determined that the variance in charge transport is not negligible when measuring the Fano factor for a semiconductor, in particular, for CdZnTe. It is argued that those variances in charge transport seen in CdZnTe are a combination of effects due to variations in carrier mobility, carrier lifetime, and electric field. It is also argued that the Fano factor carries with it a dependence on material quality as illustrated in Eq. (22). In effect, the Fano factor and electron drift length variance values are indicators of material quality. It was shown that charge transport variances are

indeed not negligible for CdZnTe, which has important implications for the materials technology of CdZnTe.

Finally, a method for determining the value of each component of signal variance was described and is applicable to

any semiconductor under certain requisite experimental conditions. The assumptions made in Eqs. (12) and (13) require that the x-ray interaction region be confined to a small area that is very near the cathode of a planar, intrinsic device.

-
- ¹U. Fano, Phys. Rev. **72**, 26 (1947).
²N. Stokan, V. Ajdacic, and B. Lalovic, Nucl. Instrum. Methods **94**, 147 (1971).
³K. G. McKay, Phys. Rev. **84**, 829 (1951).
⁴W. G. Pfann and W. van Roosbroeck, J. Appl. Phys. **25**, 1422 (1954).
⁵J. Lindhard and V. Nielsen, Phys. Lett. **2**, 209 (1962).
⁶S. O. W. Antman, D. A. Landis, and R. H. Pehl, Nucl. Instrum. Methods **40**, 272 (1966).
⁷P. Siffert, A. Coche, and F. Hibou, IEEE Trans. Nucl. Sci. **NS-13**, 225 (1966).
⁸H. M. Mann, H. R. Bilger, and I. S. Sherman, IEEE Trans. Nucl. Sci. **NS-13**, 252 (1966).
⁹H. R. Bilger, Phys. Rev. **163**, 238 (1967).
¹⁰C. A. Klein, J. Appl. Phys. **39**, 2029 (1968).
¹¹*Semiconductor Detectors*, edited by G. Bertolini and A. Coche (Wiley, New York, 1968), pp. 75–99.
¹²J. M. Palms, P. Venugopala Rao, and R. E. Wood, Nucl. Instrum. Methods **76**, 59 (1969).
¹³E. Antoncik, G. Di Cola, and L. Farese, Radiat. Eff. **5**, 1 (1970).
¹⁴J. E. Eberhardt, R. D. Ryan, and A. J. Tavendale, Appl. Phys. Lett. **17**, 427 (1970).
¹⁵E. Antoncik, Radiat. Eff. **7**, 275 (1971).
¹⁶J. E. Eberhardt, R. D. Ryan, and A. J. Tavendale, Nucl. Instrum. Methods **94**, 463 (1971).
¹⁷W. E. Drummond and J. L. Moll, J. Appl. Phys. **42**, 5556 (1971).
¹⁸E. Antoncik, J. Appl. Phys. **44**, 4778 (1973).
¹⁹T. Yamaya, R. Asano, H. Endo, and K. Umeda, Nucl. Instrum. Methods **159**, 181 (1979).
²⁰T. Papp, M.-C. Lepy, J. Plagnard, G. Kalinka, and E. Papp-Szabo, X-Ray Spectrom. **34**, 106 (2005).
²¹J. E. Eberhardt, R. D. Ryan, and A. J. Tavendale, Appl. Phys. Lett. **17**, 427 (1970).
²²J. E. Eberhardt, R. D. Ryan, and A. J. Tavendale, Nucl. Instrum. Methods **94**, 463 (1971).
²³A. Niemelä and H. Sipilä, IEEE Trans. Nucl. Sci. **41**, 1054 (1994).
²⁴G. W. Fraser, A. F. Abbey, A. Holland, K. McCarthy, A. Owens, and A. Wells, Nucl. Instrum. Methods Phys. Res. A **350**, 368 (1994).
²⁵A. Pansky, A. Breskin, and R. Chechik, J. Appl. Phys. **79**, 8892 (1996).
²⁶P. Lechner, R. Hartmann, H. Soltau, and L. Struder, Nucl. Instrum. Methods Phys. Res. A **377**, 206 (1996).
²⁷A. Owens, G. W. Fraser, A. F. Abbey, A. Holland, K. McCarthy, A. Keay, and A. Wells, Nucl. Instrum. Methods Phys. Res. A **382**, 503 (1996).
²⁸B. G. Lowe, Nucl. Instrum. Methods Phys. Res. A **399**, 354 (1997).
²⁹R. H. Redus, J. A. Pantazis, A. C. Huber, V. T. Jordanov, J. F. Butler, and B. Apotovsky, in *Semiconductors for Room-Temperature Radiation Detection Applications II*, MRS Symposia Proceedings No. 487 (Materials Research Society, Pittsburgh, 1998), pp. 101–107.
³⁰F. Perotti and C. Fiorini, Nucl. Instrum. Methods Phys. Res. A **423**, 356 (1999).
³¹T. Papp, M.-C. Lepy, J. Plagnard, G. Kalinka, and E. Papp-Szabo, X-Ray Spectrom. **34**, 106 (2005).
³²R. Devanathan, L. R. Corrales, F. Gao, and W. J. Weber, Nucl. Instrum. Methods Phys. Res. A **565**, 637 (2006).
³³B. G. Lowe and R. A. Sareen, Nucl. Instrum. Methods Phys. Res. A **576**, 367 (2007).
³⁴A. E. Bolotnikov, G. S. Camarda, G. A. Carini, Y. Cui, L. Li, and R. B. James, Nucl. Instrum. Methods Phys. Res. A **579**, 125 (2007).